EVOLUTIONS OF PLANAR POLYGONS

ALFRED M. BRUCKSTEIN
Department of Computer Science
Technion, Haifa 32000, Israel

GUILLERMO SAPIRO*
Hewlett Packard Labs., Paola Alto, CA 94304, USA

DORON SHAKED*
Hewlett-Packard, Israel Science Center,
Technion City, Haifa 32000, Israel

Evolutions of closed planar *polygons* are studied in this work. In the first part of the paper, the general theory of linear polygon evolutions is presented, and two specific problems are analyzed. The first one is a polygonal analog of a novel *affine-invariant* differential curve evolution, for which the convergence of planar curves to ellipses was proved. In the polygon case, convergence to polygonal approximation of ellipses, *polygonal ellipses*, is proven. The second one is related to cyclic pursuit problems, and convergence, either to *polygonal ellipses* or to *polygonal circles*, is proven. In the second part, two possible polygonal analogues of the well-known *Euclidean curve shortening flow* are presented. The models follow from geometric considerations. Experimental results show that an arbitrary initial polygon converges to either regular or irregular polygonal approximations of circles when evolving according to the proposed Euclidean flows.

Keywords: Planar polygons, Euclidean flows.

1. INTRODUCTION

The theory of curve evolution was studied in many different areas such as differential geometry,[18,20,31,38] parabolic equations theory,[3,4] numerical analysis,[28] computer vision,[24,30,33] and image processing.[1,29] One of the most famous studied flows is the one where the planar curve deforms in the direction of the Euclidean normal, with speed equal to the Euclidean curvature. Formally, let $\mathcal{C}(p,t) : S^1 \times [0,\tau) \to \mathbf{R}^2$ be a family of smooth simple curves in the plane, where $p \in S^1$ parameterizes the curve, and $t \in [0,\tau)$ parameterizes the family. Assume that this family of curves evolves according to the evolution equation

$$\begin{cases} \dfrac{\partial \mathcal{C}(p,t)}{\partial t} = \dfrac{\partial^2 \mathcal{C}(p,t)}{\partial v^2} = \kappa(p,t)\vec{\mathcal{N}}(p,t) \\ \mathcal{C}(p,0) = \mathcal{C}_0(p), \end{cases} \tag{1}$$

where v is the *Euclidean arc-length*, κ the *Euclidean curvature*, and $\vec{\mathcal{N}}$ the *inward unit normal*.[10] The flow given by (1) is called the *Euclidean shortening flow*, since the curve perimeter shrinks as fast as possible when the curve evolves according to

*Work done while at the Department of Electrical Engineering, Technion, Haifa, Israel.

International Journal of Pattern Recognition and Artificial Intelligence Vol. 9 No. 6 (1995) 991–1014

it.[21] Gage and Hamilton [18] proved that a simple and smooth convex curve evolving according to (1), converges to a round point. Grayson [20] proved that an embedded planar curve converges to a simple convex curve when evolving according to (1). Therefore, any embedded curve in the plane converges to a round point when it evolves according to (1).

Recently, Sapiro and Tannenbaum,[31] introduced a new curve evolution equation, the *affine shortening flow*:

$$\begin{cases} \dfrac{\partial \mathcal{C}(p,t)}{\partial t} = \dfrac{\partial^2 \mathcal{C}(p,t)}{\partial s^2} \\ \mathcal{C}(p,0) = \mathcal{C}_0(p), \end{cases} \tag{2}$$

where s is the *affine arc-length* (i.e. the simplest affine invariant of the curve),[22,31] and $\frac{\partial^2 \mathcal{C}}{\partial s^2}$ is the *affine normal*.[22] This evolution is the affine analog of Eq. (1),[31] and admits affine invariant solutions, i.e. if a family $\mathcal{C}(p,t)$ of curves, solves (2), the family obtained from it via an affine mapping, is a solution as well. Sapiro and Tannenbaum also proved that any simple and smooth convex curve evolving according to (2), converges to an ellipse.[31] They presented the natural extension of the flow (2) for non-convex initial curves as well.[32] In this case, they proved that the curve first becomes convex, as in the Euclidean case, and after that it converges into an ellipse according to the results in Ref. 31.

Motivated by the search for discrete versions of these theorems, the evolution of planar polygons is studied in this paper. The first part of this paper is dedicated to the development of a general theory of linear evolutions, i.e. evolutions governed by matrix transformations. When this matrix is real, such evolutions are automatically affine invariant. As examples, a polygonal analog of the affine shortening flow, and a model of polygonal cyclic pursuit, are presented.

Since linear models cannot bring forth a polygonal analog of the Euclidean shortening flow, the goal of the second part of the paper is to present possible non-linear analogues. Particularly, two models are presented and experimentally studied. The first model is based on a definition of polygonal Euclidean curvature. The second model is derived from the polygonal analog of the affine shortening flow.

This paper is organized as follows: Section 2 deals with the linear theory. Section 2.1 presents the general theory of linear polygon evolution. Section 2.2 deals with a polygonal analog of Eq. (2), and proves convergence to a *polygonal ellipse* (a polygonal approximation of an ellipse). Section 2.3 deals with a polygonal evolution related to cyclic pursuit, and proves convergence either to a *polygonal ellipse* or to a *polygonal circle*. Section 3 deals with the possible non-linear analogues of the Euclidean shortening flows. Section 3.1 presents the first model. The model derived from the polygonal affine evolution is given in Sec. 3.2. Concluding remarks are given in Sec. 4.

2. LINEAR POLYGONAL EVOLUTIONS

In this section, a general model of linear evolutions of planar polygons is presented and analyzed. Two examples are discussed.

2.1. The General Model

Let P be a planar polygon with N vertices. P may be non-convex and self intersecting. Each one of the vertices P_i of P, $i = 0, 1, \ldots, N-1$, can be represented by a point in the complex plane. Therefore, the polygon P is an N-dimensional vector over the complex field C: $P = [P_0, P_1, \ldots, P_{N-1}]^T$, $P_i \in C$. A linear evolution of the polygon is described by

$$\begin{cases} P(n) = MP(n-1) \\ P(0) = P \end{cases} \tag{3}$$

where M is a constant $N \times N$ complex matrix, and $n \in \mathbf{N}^+$ is the discrete time. In the evolution described by Eq. (3), the coordinates of each polygon vertex are obtained by a linear combination of the coordinates of the previous polygon. Note that the number of vertices is constant in the evolution process.

An *affine* mapping of a point $X = [x, y]^T$ in R^2 (or $X = (x + jy)$ in C) is given by

$$\tilde{X} = AX \tag{4}$$

where A is a 2×2 non-singular real matrix (the *affine matrix*).[7,22] The linear polygonal evolution given by Eq. (3), is affine invariant[7,22] if M is real, i.e. if the points of $P(n)$ and $\tilde{P}(n)$ are related by an affine mapping, and $P(n)$ evolves according to (3), $\tilde{P}(n)$ also evolves according to (3). When a translation vector $V_{2\times 1}$ is added in Eq. (4), the solution of the evolution equation must be translated also.

Assuming that all vertices of P evolve according to the same rule, the evolution matrix M must be *circulant*.[19] Therefore, M is well defined by its first row $m_{1\times N}$ (all other rows are circular shifts of m). A well-known property of circulant matrices[19] is that they can be decomposed as follows

$$M = U \Lambda U^{-1} \tag{5}$$

where U is an orthogonal matrix such that its i-column, $i = 0, 1, \ldots, N-1$, is given by

$$W^i = [w^0, w^i, w^{2i}, \ldots, w^{i(N-1)}]^T, \quad w^i = \exp\left\{j\frac{2\pi i}{N}\right\}, \quad j = \sqrt{-1}$$

and Λ is a diagonal matrix

$$\Lambda = diag\{\lambda_i\}$$

where λ_i is the ith eigenvalue of M

$$\lambda_i = N \cdot IDFT_i(m) = mW^i$$

Here, $IDFT_i(\cdot)$ stands for the ith element of the Inverse Discrete Fourier Transform. It can be shown that $U^{-1} = \frac{1}{N}U^*$ (U^* stands for the conjugate transpose of U).[19]

From (3) and (5) we obtain

$$P(n) = M^n P = \frac{1}{N} U \Lambda^n U^* P = \frac{1}{N} \sum_{i=0}^{N-1} (\lambda_i)^n W^i (W^i)^* P$$
$$= \frac{1}{N} \sum_{i=0}^{N-1} (\lambda_i)^n DFT_i(P) W^i$$

Since we are interested in evolutions confined to a finite region in R^2, Λ^n must remain bounded. Thus the matrix M should be scaled to yield

$$\max \{|\lambda_i|\} \le 1$$

Consider the set of indices

$$l(m) \triangleq \{i : |\lambda_i| = 1\}$$

and define

$$P^\infty(n) \triangleq \frac{1}{N} \sum_{l(m)} \exp\{jn \arg(\lambda_i)\} W^i (W^i)^* P$$
$$= \frac{1}{N} \sum_{l(m)} \exp\{jn \arg(\lambda_i)\} DFT_i(P) W^i$$

where $\arg(x)$ stands for the complex argument of x.

$P(n)$ converges to $P^\infty(n)$ in the sense that $\lim_{n\to\infty} |P_i(n) - P_i^\infty(n)| = 0$ for $i = 0, 1, \ldots, N-1$.

If $i \neq 0$, $i \in l(m)$, exists, then $P(n)$ converges to the polygon $P^\infty(n)$, whose shape depends on the elements of $l(m)$.

If $l(m) = \emptyset$, $P^\infty(n) = \mathbf{0}$. If $l(m) = \{0\}$, $P^\infty(n) = \exp\{jn \arg(\lambda_0)\}\bar{P}$, where $\bar{P} = \left(\frac{1}{N}\sum_{i=0}^{N-1} P_i\right)[1, 1, \ldots, 1]^T$ (center of mass of the initial polygon). In both cases, the limiting polygon $P^\infty(n)$ is a point, and the interest shifts to the shape $P(n)$ takes while approaching $P^\infty(n)$. In order to investigate this, the polygon $P(n)$ is normalized as follows

$$B(n) \triangleq \frac{1}{N\alpha^n(m)} \sum_{i \notin l(m)} (\lambda_i)^n W^i (W^i)^* P$$
$$= \frac{1}{N\alpha^n(m)} \sum_{i \notin l(m)} (\lambda_i)^n DFT_i(P) W^i$$

where

$$\alpha(m) \triangleq \max_{i \notin l(m)} \{|\lambda_i|\}$$

If

$$b(m) \triangleq \{i : |\lambda_i| = \alpha(m)\}$$

then

$$B^\infty(n) \triangleq \frac{1}{N} \sum_{b(m)} \exp\{jn \arg(\lambda_i)\} DFT_i(P) W^i \tag{6}$$

and $B^\infty(n)$ provides the geometric behavior of the polygon when $n \to \infty$ (i.e. when $P(n)$ converges to $P^\infty(n)$). From Eq. (6) it is clear that the shape of the polygon, when converging to $P^\infty(n)$, is governed by the second greatest eigenvalues.

In what follows, we assume that $P^\infty(n)$ is a point (i.e. $l(m) = \emptyset$ or $l(m) = \{0\}$), and investigate $B^\infty(n)$. If $P^\infty(n)$ is not a point, $P^\infty(n)$ can be analyzed in a similar way as $B^\infty(n)$ (see Sec. 2.3 for an example).

Definition 2.1. A polygon Q is a *polygonal circle of radius* r ($r \in R^+$), if all its points belong to a circle of radius r, and Q has no self intersections. A polygonal circle is a polygonal approximation of a circle $\mathcal{C}$ of radius r.

Definition 2.2. A polygon Q is a *polygonal ellipse* if all its points belong to an ellipse, and Q has no self intersections. A polygonal ellipse is a polygonal approximation of an ellipse $\mathcal{E}$.

Theorem 2.1. If $b(m) = \{1\}$, and $DFT_1(P) \neq 0$, then $B^\infty(n)$ is a polygonal circle.

Proof. Let $\frac{1}{N}e^{jn\arg(\lambda_1)}DFT_1(P) = ae^{j\psi(n)}$ ($a \neq 0$), and $\theta_i \triangleq \frac{2\pi}{N}i$ ($i = 0, 1, \ldots, N-1$). Then, from Eq. (6)

$$B^\infty(n) = ae^{j\psi(n)}W^1$$

Since $W^1 = [e^{j\theta_i}]$ is a polygonal circle of radius 1, $B^\infty(n) = \left[ae^{j(\psi(n)+\theta_i)}\right]$ is a polygonal circle of radius a (see Fig. 1). □

Note that $B^\infty(n)$ is a rotating polygonal circle with constant radius a. $B^\infty(n+1)$ is obtained from $B^\infty(n)$ by a rotation of $arg(\lambda_1)$.

Corollary 2.2. If $b(m) = \{N-1\}$, and $DFT_{N-1}(P) \neq 0$, then $B^\infty(n)$ is a polygonal circle.

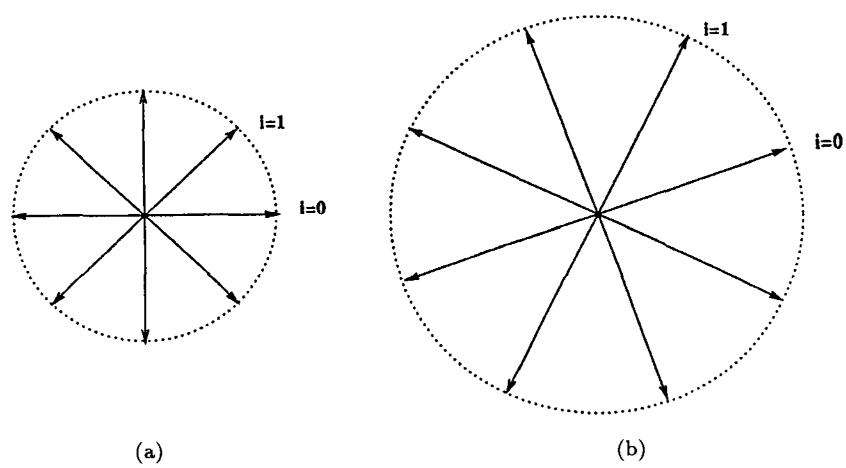

Fig. 1. Example of a polygonal circle (Theorem 2.1): (a) The vector W^1 (for $N = 8$). This is a polygonal circle of radius 1. (b) The vector W^1 magnified by a factor $a > 1$ and rotated.

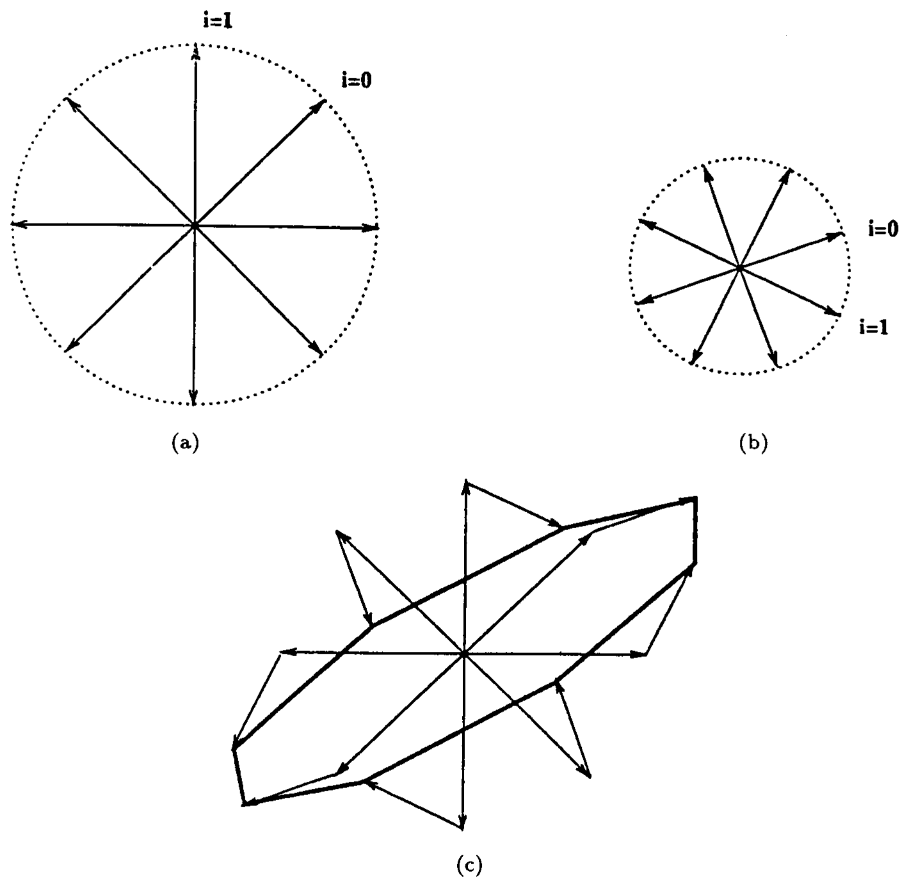

Fig. 2. How to obtain a polygonal ellipse (Theorem 2.3): (a) The vector $AW^1 (A = ae^{\psi 1})$. (b) The vector $BW^{-1} (B = be^{\psi 2}$, note that i increases clockwise). (c) The polygonal ellipse is obtained by vector addition (with corresponding index) of the figures in (a) and (b).

Theorem 2.3. If $b(m) = \{1, N-1\}$, and $DFT_1(P) \neq 0$, or $DFT_{N-1}(P) \neq 0$, then $B^\infty(n)$ is a polygonal ellipse.

Proof. Let $\frac{1}{N}e^{jn\arg(\lambda_1)}DFT_1(P) = ae^{j\psi_1(n)}$, and $\frac{1}{N}e^{jn\arg(\lambda_{N-1})}DFT_{N-1}(P) = be^{j\psi_2(n)}$ (note that a and b are independent of n). Then, from Eq. (10)

$$B^\infty(n) = ae^{\psi_1(n)}W^1 + be^{\psi_2(n)}W^{-1}$$

Define $\bar{\psi}(n) \triangleq \frac{\psi_1(n)+\psi_2(n)}{2}$ and $\psi(n) \triangleq \frac{\psi_1(n)-\psi_2(n)}{2}$. Then,

$$ae^{\psi_1} = ae^{j\psi}e^{j\bar{\psi}}$$
$$be^{\psi_2} = be^{-j\psi}e^{j\bar{\psi}}$$

The vectors W^1 and W^{-1} can be written as

$$W^1 = [w^i] = [e^{j\frac{2\pi i}{N}}] = [e^{j\theta_i}] = [\cos(\theta_i) + j\sin(\theta_i)]$$

$$W^{-1} = [w^{-i}] = [e^{-j\frac{2\pi i}{N}}] = [e^{-j\theta_i}] = [\cos(\theta_i) - j\sin(\theta_i)]$$

and

$$\begin{aligned} ae^{j\psi}w^i + be^{-j\psi}w^{-i} &= ae^{j(\psi+\theta_i)} + be^{-j(\psi+\theta_i)} \\ &= (a+b)\cos(\psi+\theta_i) + j(a-b)\sin(\psi+\theta_i) \end{aligned}$$

Those points belong to an ellipse of radii $(a+b)$ and $(a-b)$ (Fig. 2). Since $e^{j\bar{\psi}}$ just rotates the polygon, the points of $B^\infty(n) = e^{j\bar{\psi}}[ae^{j\psi}w^i + ae^{-j\psi}w^{-i}]$ also belong to an ellipse.

Let $\xi_i(n)$ be the angle between the horizontal axis and the vector defined by the ith point of $B^\infty(n)$. From the last equation

$$\tan(\xi_i - \bar{\psi}) = \frac{a-b}{a+b}\tan(\psi + \theta_i)$$

The fact that $B^\infty(n)$ has no self intersections follows directly from the monotonic property of $\tan(\cdot)$. Therefore, $B^\infty(n)$ is a polygonal ellipse. □

Remark 2.1. In Theorem 2.3, $B^\infty(n)$ approximates an ellipse $\mathcal{E}(n)$ with constant shape (radii $(a+b)$ and $(a-b)$), and rotating axes. The rotation angle of $\mathcal{E}(n)$ is given by $\bar{\psi}(n)$. The vertices of $B^\infty(n)$ rotate on $\mathcal{E}(n)$. The rotation angle on $\mathcal{E}(n)$ is given by $\psi(n)$. If the evolution matrix M is real, it can be shown that $\bar{\psi}(n) = constant$, and $\mathcal{E}(n)$ does not rotate, i.e. $\mathcal{E}(n) = \mathcal{E}$ for all n. Furthermore, if λ_1 and λ_{N-1} are real, $B^\infty(n)$ does not rotate on $\mathcal{E}$.

Remark 2.2. Condition (2) of the above theorems holds for almost all initial polygons P. In case it does not hold, the convergence is dominated by the next greatest eigenvalues and similar analysis can be performed.

Remark 2.3. Results similar to the theorems above can readily be formulated for $P(n)$, replacing $b(m)$ and $B^\infty(n)$ by $l(m)$ and $P^\infty(n)$, respectively.

2.2. Affine Polygonal Shortening

In this section, a polygonal version of the *affine curve evolution* (Eq. (2)[31]), is presented and studied.

Let $P(p,n)$ be the coordinates of a point p of the polygon P after n iterations of the polygon evolution process (Eq. (3)). The discrete version of Eq. (2) is given by

$$\begin{aligned} P(p,n+1) - P(p,n) &= \frac{c}{2}\{[P(s+1,n) - P(s,n)] - [P(s,n) - P(s-1,n)]\} \\ &= \frac{c}{2}\{P(s+1,n) - 2P(s,n) + P(s-1,n)\} \end{aligned}$$

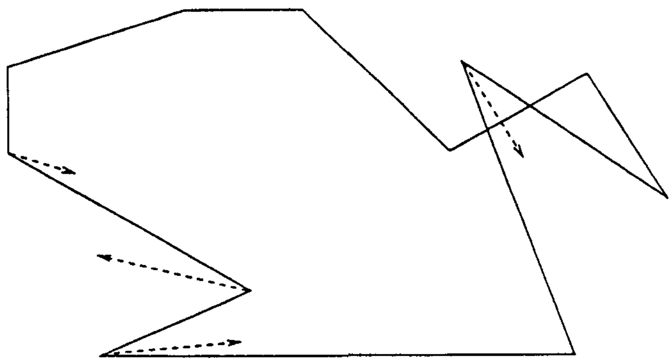

Fig. 3. Geometry of the affine poygon evolution (Sec. 2.2). The dashed lines show the evolution direction of the vertices (local center of mass).

where c is a real constant. Set the parameterization p of the polygon P to be consecutive integers (modulo N) at the vertices, so that for $i \in \{0, 1, \ldots, N-1\}$, $P(i,n) \equiv P_i(n)$. Since polygon vertices (i.e. curve breakpoints) are affine invariant, the discrete affine arc-length s can be chosen so that at the ith vertex $s = i$. With this selection, we obtain the following evolution equation for the polygon vertices:

$$P_i(n+1) = (1-c)P_i(n) + \frac{c}{2}P_{i-1}(n) + \frac{c}{2}P_{i+1}(n) \tag{7}$$

This equation describes a linear transformation and corresponds to the following selection of the first row m of the matrix M in Eq. (3)

$$m = \left[1-c,\ \frac{c}{2},\ 0,\ \ldots,\ 0,\ \frac{c}{2}\right] \tag{8}$$

The geometric interpretation of this transformation is as follows: As c goes from 0 to $\frac{2}{3}$, the point $P_i(n)$ goes from its previous position $P_i(n-1)$ to the local center of mass of the points P_i, P_{i-1}, P_{i+1} at time $(n-1)$. Therefore, the evolution of a polygon vertex is a step towards the local weighted center of mass (see Fig. 3).

Remark 2.4. For general curves, the affine arc-length is a non-linear function of the parameter p,[22,31] and as a result we obtain that the affine evolution (2) is a non-linear PDE. In the polygonal evolution presented above, s is a linear function of p at the vertices ($s \equiv p$), and therefore the evolution obtained is a linear transformation on the vertices.

We now proceed to analyze the above polygonal evolution by means described in Sec. 2.1. For the m in Eq. (8) we obtain

$$\begin{aligned}\lambda_i = mW^i &= \sum_{k=0}^{N-1} m_k \exp\{j2\pi ik/N\} \\ &= 1 - c + c\left[\cos\left(\frac{2\pi i}{N}\right)\right]\end{aligned}$$

It is clear that in this case $\lambda_i \in R$ for all i, max $\{|\lambda_i|\} = \lambda_0 = 1$, and

$$l(m) = \{0\}$$

Therefore, the polygon $P(n)$ converges to the global center of mass $\bar{P}$ of the initial polygon P.

In order to learn about the shape of $P(n)$ while converging to $\bar{P}$, we find $B^\infty(n)$ (Eq. (6)). The first step consists of computing $\alpha(m)$, i.e. the maximal value of $|\lambda_i|$ such that $i \notin l(m)$. Since $\lambda_i \in R$ and receives both positive and negative values,

$$\max\{|\lambda_i|\} = \max\{\max\{\lambda_i\}\ ,\ -\min\{\lambda_i\}\}$$

From the general expression for λ_i,

$$\max\{\lambda_i\} = \lambda_1 = \lambda_{N-1} = 1 - c + c\left[\cos\left(\frac{2\pi}{N}\right)\right]$$

$$\min\{\lambda_i\} = \begin{cases} \lambda_{N/2} & \text{N even} \\ \lambda_{\frac{N-1}{2}} = \lambda_{\frac{N+1}{2}} & \text{N odd} \end{cases}$$

$$= \begin{cases} 1 - c + c[\cos(\frac{2\pi}{N}\frac{N}{2})] & \text{N even} \\ 1 - c + c[\cos(\frac{2\pi}{N}\frac{N-1}{2})] & \text{N odd} \end{cases}$$

$$= \begin{cases} 1 - 2c & \text{N even} \\ 1 - c - c[\cos(\frac{\pi}{N})] & \text{N odd} \end{cases}$$

In the last equation, $c > \frac{1}{2}$ for N even, and $c > \frac{1}{1+\cos\frac{\pi}{N}}$ for N odd (otherwise λ_i is not negative).

We now proceed to show that for all $N > 2$,

$$\max\{\lambda_i\}\ \geq\ -\min\{\lambda_i\} \tag{9}$$

It can be shown that if inequality (9) holds for a pair (N^*, c^*), it also holds for any other pair (N, c) such that $N \geq N^*$ and $c \leq c^*$. Therefore, we have to find the minimal N and the maximal c such that (9) holds. Remember that $N > 2$ and $0 < c \leq \frac{2}{3}$.

1. For $N = 3$ (the minimal value), and for all $c \leq \frac{2}{3}$, we obtain that $\lambda_1 = \lambda_2 > 0$.
2. For $c = \frac{2}{3}$ (the largest c), and $N = 5$ (the smallest odd N after 3), we obtain

$$\lambda_1 = \lambda_4 = 1 - \frac{2}{3} + \frac{2}{3}\cos\left(\frac{2\pi}{5}\right)$$

$$\lambda_2 = \lambda_3 = 1 - \frac{2}{3} - \frac{2}{3}\cos\left(\frac{\pi}{5}\right)$$

$$\lambda_1 = \lambda_4 > |\lambda_2| = |\lambda_3|$$

and (9) holds.

3. For $N = 4$ (the smallest even N) and $c = \frac{2}{3}$,

$$\lambda_1 = \lambda_3 = 1 - \frac{2}{3} + \frac{2}{3}\cos\left(\frac{2\pi}{4}\right) = \frac{1}{3}$$
$$\lambda_2 = -\frac{1}{3}$$
$$\lambda_1 = \lambda_3 = |\lambda_2|$$

and (9) holds.

We conclude that

1. For $N = 4$,

$$\alpha(m) = \frac{1}{3}$$
$$b(m) = \{1, 2, 3\}$$

and $B^\infty(n)$ depends on all the vectors W^i, $i \neq 0$.

2. For all $N \neq 4$ and $0 < c \leq \frac{2}{3}$,

$$\alpha(m) = 1 - c + c\left[\cos\left(\frac{2\pi}{N}\right)\right]$$
$$b(m) = \{1,\ N-1\}$$

Since $\arg(\lambda_1) = \arg(\lambda_{N-1}) = 0$, B^∞ is given by (Eq. (6))

$$B^\infty = \frac{1}{N}DFT_1(P)W^1 + \frac{1}{N}DFT_{N-1}(P)W^{N-1} \tag{10}$$

Theorem 2.4. Let $P(n)$ be a polygon evolving according to the evolution Eq. (8), with $P(0) = P$. If

1. $N \neq 4$ and $0 \leq c \leq \frac{2}{3}$
2. $DFT_1(P) \neq 0$ or $DFT_{N-1}(P) \neq 0$

then $P(n)$ converges to $\bar{P}$ (center of mass of the initial polygon), and the normalized polygon $B^\infty(n)$ converges to a fixed polygonal ellipse.

Proof. Since $l(m) = \{0\}$ and $\arg(\lambda_0) = 0$, $P^\infty(n) = \bar{P}$. For $N \neq 4$, and $0 \leq c \leq \frac{2}{3}$, we obtained that $b(m) = \{1,\ N-1\}$. From Theorem 2.3, $B^\infty(n)$ converges to a polygonal ellipse. Since M, λ_1, and λ_{N-1}, are all real, $B^\infty(n)$ does not rotate, i.e. $B^\infty(n) = B^\infty$ for all n (see Remark 2.1). □

Remark 2.5. B^∞ is independent of the selection of the parameter c (as long as $c \in \left[0, \frac{2}{3}\right]$). This parameter simply controls the speed of convergence.

The result in Theorem 2.4 is not unexpected, since as previously explained, this evolution is a polygonal version of the affine curve evolution studied in Ref. 31. See Figs. 4 and 5 for evolution examples.

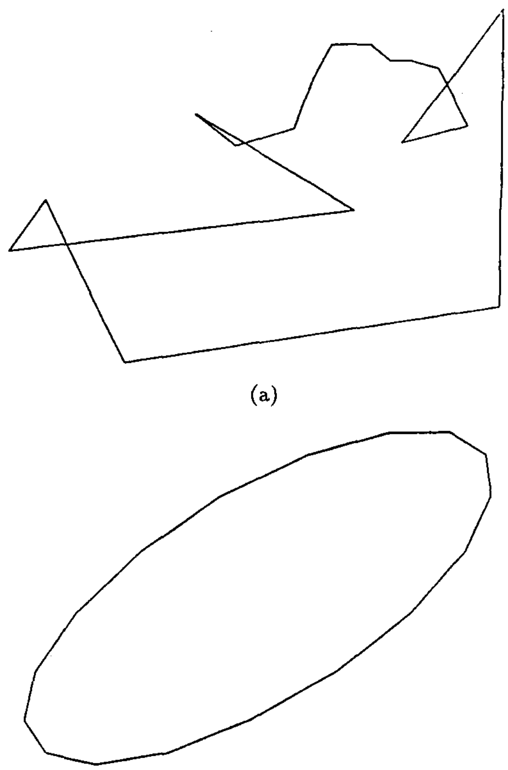

(a)

(b)

Fig. 4. A simple affine evolution example: (a) The initial polygon P. (b) The limit normalized polygon (B^{∞}): a polygonal ellipse.

2.3. Polygonal Cyclic Pursuit

In this section we study the limit shape of the linear polygonal cyclic pursuit. The cyclic pursuit problem is a particular case of polygonal evolution problems, in which every vertex moves towards the next vertex. Several such problems were studied by Bruckstein *et al.*,[8] addressing non-linear evolution rules and the question of convergence.

The linear polygonal cyclic pursuit is given by:

$$P_i(n+1) = (1-c)P_i(n) + cP_{i+1}(n) \tag{11}$$

Equation (11) determines the first row m of the matrix M in (3)

$$m = [1-c,\, c,\, 0,\, \ldots,\, 0] \tag{12}$$

The eigenvalues of M are

$$\lambda_i = 1 - c + c\exp\left\{j\frac{2\pi i}{N}\right\}$$

In this case, it is clear that λ_i is not real.

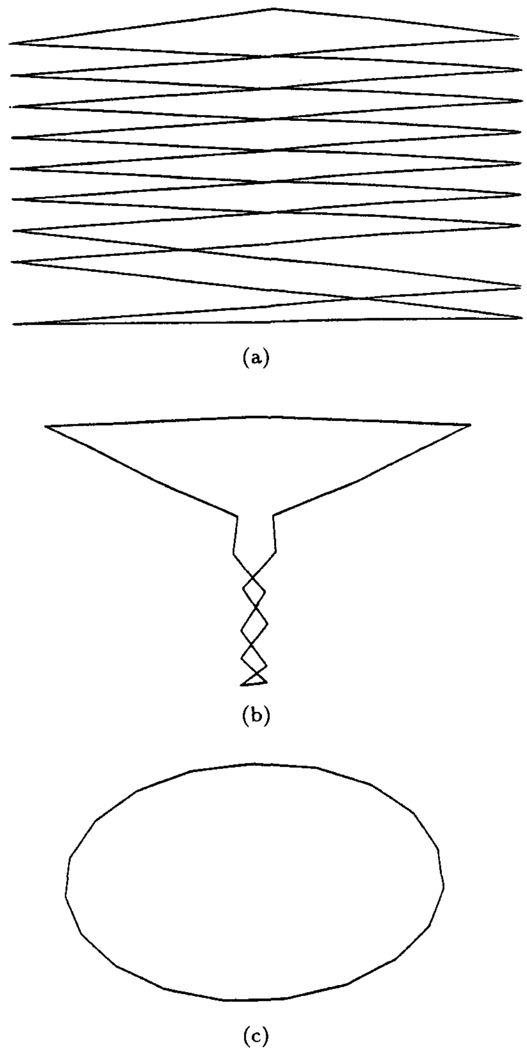

Fig. 5. A more complicated affine evolution example: (a) The initial polygon P. (b) The normalized polygon $(B(n))$ after 40 iterations. (c) The limit normalized polygon (B^{∞}).

Assume first that c in (11) is real and $c \in [0, \frac{1}{2}]$. In this case, the vertex P_i evolves towards the next one. The eigenvalues λ_i are located on a circle in the complex plane. The circle is of radius c, centered at the point $1 - c$ (see Fig. 6). It is clear that

1. $|\lambda_i| \leq 1$ for all i
2. $l(m) = \{0\}$
3. $\alpha(m) = \left|1 - c\left(1 - \exp\left\{j\frac{2\pi}{N}\right\}\right)\right|$
4. $b(m) = \{1, N-1\}$

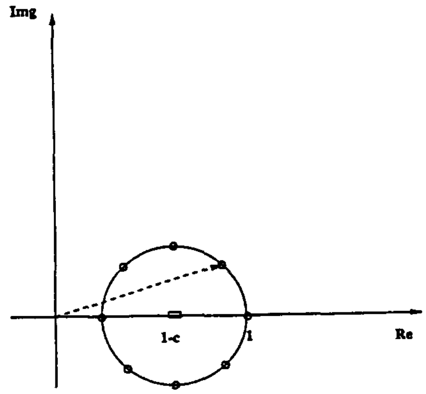

Fig. 6. Eignevalues of the polygonal cyclic pursuit with real evolution matrix ($c \in R$, Sec. 2.3). The eigenvalues (denoted by a small circle) are on a circle, and their magnitude is less or equal to 1.

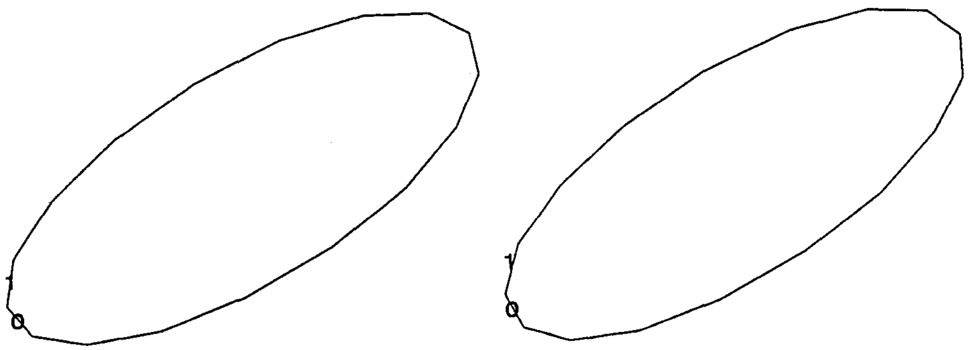

(a) (b)

Fig. 7. Example of polygonal cyclic pursuit with $c \in C$. The initial polygon is given in Fig. 4(a). (a) The limit normalized polygon ($B^{\infty}(n)$). (b) The limit normalized polygon after one more iteration. Note that $B^{\infty}(n+1)$ approximates the same ellipse as $B^{\infty}(n)$.

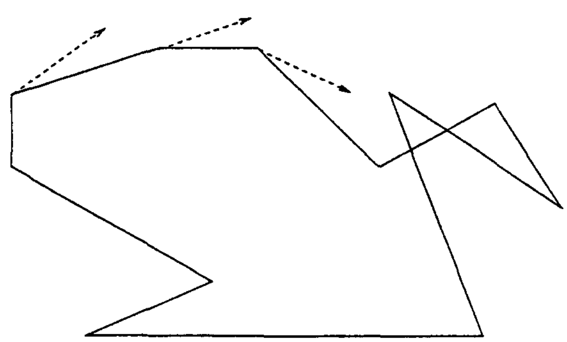

Fig. 8. The geometry of the complex polygonal cyclic pursuit ($c \in C$, Sec. 2.3). The vertex makes small rotation before "jumping" (dashed line).

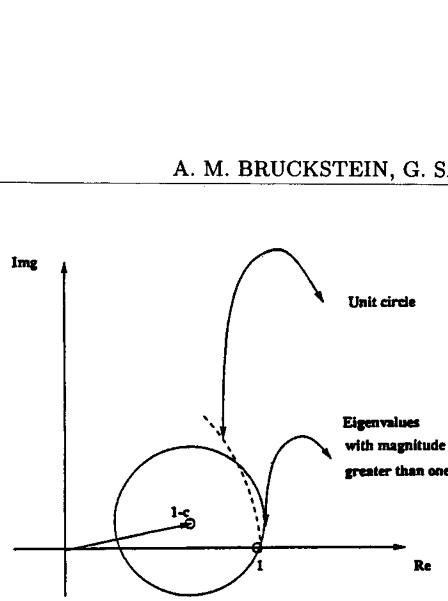

Fig. 9. Eigenvalues of the polygonal cyclic pursuit with complex evolution matrix ($c \in C$). All the eigenvalues are on the circle, and the magnitude of some of them can be greater than 1.

Therefore, $P^\infty(n) = \bar{P}$, and if the corresponding Fourier coefficients of the initial polygon are not zero, $B^\infty(n)$ is a polygonal ellipse (see Theorem 2.3). Since M is real, $B^\infty(n)$ approximates a non-rotating ellipse $\mathcal{E}$. In contrast with the affine polygonal evolution, $B^\infty(n)$ rotates on $\mathcal{E}$ (Remark 2.1). Figure 7 presents an example of this pursuit problem.

An interesting case of polygonal cyclic pursuit is when the constant c in Eq. (11) is a complex number (note that when M is not real, the evolution ceases to be affine invariant). The geometric interpretation is as follows: Each vertex "looks" at the next vertex and instead of "going" on a straight line between them, it makes a little rotation before "jumping" (see Fig. 8). A problem of this type was studied by M. Klamkin[25] for the case where P is the unit square. In the general case, the eigenvalues of the matrix M are located on a circle of radius $|c|$ around the complex center point $(1-c)$. As in the previous case, $\lambda_0 = 1$, but now, some eigenvalues λ_r may be larger ($|\lambda_r| > 1$, see Fig. 9). If, however, the argument of c is small enough, the matrix is stabilized ($|\lambda_i| \leq 1$ for all i). The critical argument is

$$\arg(c) = \frac{\pi}{N} - \arcsin\left[|c| \sin\left(\frac{\pi}{N}\right)\right]$$

In the critical case

$$|\lambda_0| = |\lambda_1| = 1$$

$$l(m) = \{0, 1\}$$

and

$$P^\infty(n) = \frac{1}{N} e^{jn\arg(\lambda_1)} DFT_1(P) W^1 + \bar{P}$$

Using the same arguments as in proving Theorem 2.1, we conclude that $P^\infty(n)$ is a polygonal circle, of constant radius $\frac{1}{N}|DFT_1(P)|$, rotating around $\bar{P}$ (center of mass of the initial polygon). The rotation angle is $\arg(\lambda_1)$ per iteration (see Fig. 10).

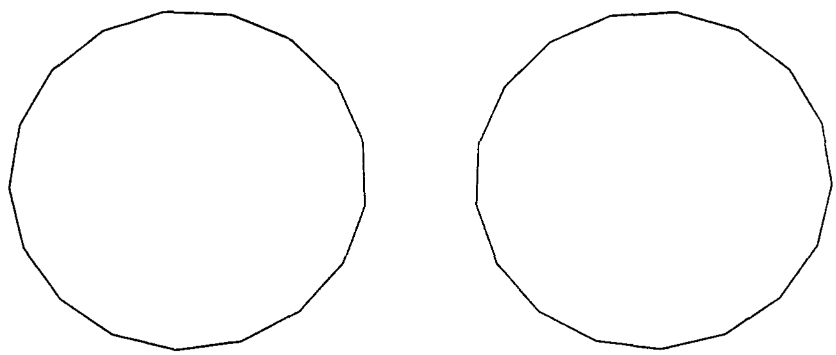

(a) (b)

Fig. 10. Example of polygonal cyclic prusuit with $c \in C$. The initial polygon is given in Fig. 4(a). (a) The limit polygon $P^{\infty}(n)$. (b) The limit polygon after one more iteration. Note that $P^{\infty}(n+1)$ approximates the same circle as $P^{\infty}(n)$.

3. EUCLIDEAN POLYGONAL SHORTENING

In the case of polygon evolution, we found an affine invariant discrete parameterization ($s \equiv p$, see Remark 2.4), that allows us to give a linear analogue of the affine shortening flow (2). In the case of Euclidean polygon evolution, the natural discrete Euclidean arc-length v, must take into account the length of the polygon sides, making the relation between this parameterization and p, non-linear. Therefore, we cannot obtain a linear Euclidean shortening analogue for polygons. We shall next present two possible non-linear analogues.

3.1. The First Model: Polygonal Curvature

In this section we present an analog of Eq. (1) which is based on a rather natural geometric definition for polygonal Euclidean curvature. This model was suggested by Prof. Sanjeev Kulkarni from Princeton University. First, recall the definition of the Euclidean curvature of a smooth planar curve[36]:

Definition 3.1. Let $\mathbf{x}$ be a non-inflection point of a smooth planar curve $\mathcal{C}$, and $\mathbf{y}$ and $\mathbf{z}$ two other points in $\mathcal{C}$. The three points $\mathbf{x}$, $\mathbf{y}$, $\mathbf{z}$, define a unique circle $\mathcal{D}_{xyz}$. When the points $\mathbf{y}$ and $\mathbf{z}$ converge to the point $\mathbf{x}$, the circle $\mathcal{D}_{xyz}$ converges to a circle $\mathcal{D}$. The *Euclidean curvature* of $\mathcal{C}$ at $\mathbf{x}$ is defined as the inverse of the radius of this limiting circle $\mathcal{D}$. The radius of $\mathcal{D}$ is called the *radius of curvature*, and its center is the *center of curvature*.

In the case of polygons, the discrete curvature at a vertex of a planar polygon P can be defined as follows:

Definition 3.2. Let P_i be a vertex of a polygon P, and P_{i-1} and P_{i+1} its two adjacent vertices (the polygon is assumed to be closed, as in Sec. 2). We define the *polygonal curvature* of P at P_i as the inverse of the radius of the circle $\mathcal{O}$ determined by the three vertices P_i, P_{i-1}, and P_{i+1}. The radius is called the *polygonal radius of curvature*, and the center is the *polygonal center of curvature.* If the three vertices are collinear, we say that the polygonal curvature at P_i is equal to zero.

Observe that when the polygon approximates more and more closely a given smooth curve, the circle $\mathcal{O}$ converges to the circle $\mathcal{D}$.

Using Definition 3.2, the polygonal analog of the Euclidean shortening flow given by Eq. (1) follows immediately. The "normal" direction is given by the vector defined from the vertex to the corresponding polygonal center of curvature, and the velocity is given by the polygonal curvature. In other words, one can define the first model for the *polygonal Euclidean shortening flow*, as the flow in which each

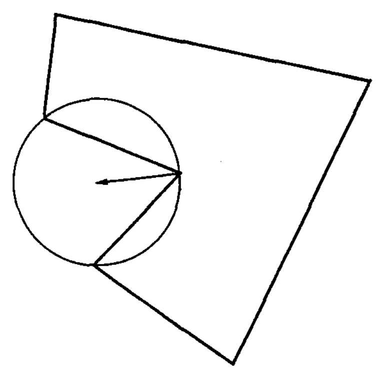

Fig. 11. Geometry of the *polygonal curvature*.

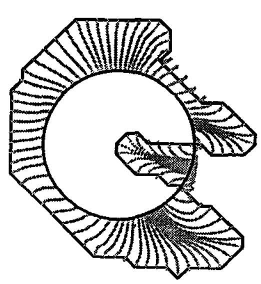

Fig. 12. Examples of the first polygonal Euclidean shortening model. The two dark lines show the initial polygon and the final one (polygonal circle). The other lines show the motion of the different vertices.

polygonal vertex moves in the direction of the polygonal center of curvature with velocity equal to the polygonal curvature (see Fig. 11).

It is easy to prove that a polygonal circle is a stable shape of the proposed polygonal flow, i.e. the normalized shape of a polygonal approximation of a circle is stationary when evolving according to the mentioned polygonal shortening flow.

This evolution was checked experimentally (see Fig. 12). All the experiments indicated that arbitrary initial polygons converged to polygonal circles.[a] Note however that the resulting polygonal circles can be rather irregular (see Fig. 12).

3.2. The Second Model: From Polygonal Affine Shortening to an Euclidean One

We next present a different possible analog of the Euclidean shortening flow (1) which is based on the polygonal analog of the affine shortening flow described in Sec. 2.2.

In Sec. 2.2, it was shown that a polygonal analog of Eq. (2) is given by vertex evolution towards local centers of mass. With this flow, each vertex P_i of the planar polygon P evolves toward the center of mass of the triangle determined by it and its two adjacent vertices P_{i-1} and P_{i+1}. See Eqs. (7) and (8).

In order to describe the second polygonal model of the Euclidean shortening flow, we shall first briefly present a classical result of the theory of curve evolution. We consider for a moment smooth plane curves deforming in time. Let $\mathcal{C}(p,t) : S^1 \times [0,\tau) \to \mathbf{R^2}$ denote a family of closed embedded curves, where t parameterizes the family, and p parameterizes each curve. Assume that this family evolves according to

$$\begin{cases} \frac{\partial \mathcal{C}}{\partial t} = \alpha \vec{\mathcal{T}} + \beta \vec{\mathcal{N}} \\ \mathcal{C}(p,0) = \mathcal{C}_0(p), \end{cases} \tag{13}$$

where $\vec{\mathcal{N}}$ is the inward Euclidean unit normal, $\vec{\mathcal{T}}$ the unit tangent,[10,36] and α, β the tangent and normal components of the evolution velocity $\vec{v}$, respectively.

In order to separate the geometric concept of a planar curve from its formal algebraic description, we define the image of $\mathcal{C}(p,t)$, denoted by $Img[\mathcal{C}(p,t)]$.[33] If the curve $\mathcal{C}(p,t)$ is parameterized by a new parameter $w(p,t)$ such that $\frac{\partial w}{\partial t} > 0$, we clearly have

$$Img[\mathcal{C}(p,t)] = Img[\mathcal{C}(w,t)].$$

The following lemma shows that under certain conditions on the flow, the tangential velocity does not affect $Img[\mathcal{C}]$.

Lemma.[14] Let β be a geometric quantity for a curve, i.e. a function whose definition is independent of a particular parameterization. Then a family of curves $\mathcal{C}(p,t)$ which evolves according to

$$\mathcal{C}_t = \alpha \vec{\mathcal{T}} + \beta \vec{\mathcal{N}}$$

[a]The polygonal radii of curvature converge to the same value, and the polygonal centers of curvature converge to the same point.

can be converted into a family of curves $\mathcal{C}(w,t)$ which evolves according to

$$\mathcal{C}_t = \bar{\alpha}\vec{\mathcal{T}} + \bar{\beta}\vec{\mathcal{N}},$$

for any continuous function $\bar{\alpha}$, by changing the space parameterization of the original solution, so that $\frac{\partial w}{\partial p} > 0$, and also $\bar{\beta}(w(p,t),t) = \beta(p,t)$.

For proofs of the lemma, see Refs. 14 and 33.

In other words, the Lemma says that if the normal component of the velocity is a geometric function of the curve, then $Img[\mathcal{C}]$ (which represents the "geometry" of the curve) is only affected by its normal component. The tangential component affects only the parameterization, and not $Img[\mathcal{C}]$ (which is independent of the parameterization by definition). Therefore, assuming that the normal component β of $\vec{v}$ (the curve evolution velocity) in (13) does not depend on the curve parameterization, we can consider the evolution equation

$$\frac{\partial \mathcal{C}}{\partial t} = \beta\vec{\mathcal{N}}, \tag{14}$$

where $\beta = \vec{v}\cdot\vec{\mathcal{N}}$, i.e. the projection of the velocity vector on the normal direction.

In Refs. 31 and 32, it was proven that the normal component of the *affine normal* C_{ss} (see Eq. (2)) is equal to $\kappa^{1/3}$. Therefore, the flow given by Eq. (2) is geometric equivalent to the flow given by

$$\mathcal{C}_t = \kappa^{1/3}\vec{\mathcal{N}}. \tag{15}$$

Going back to the polygonal case, we may argue that the polygonal evolution given by the local center of mass (Eq. (7)), which is the polygonal analog of the affine shortening flow (2), is also the polygonal analog to the flow given by Eq. (15). The advantage of "re-writing" Eq. (2) as Eq. (15) is that in the last equation, both the Euclidean curvature and normal appear. The evolution towards the local center of mass is then a polygonal analog to the evolution in the direction to the Euclidean normal, with velocity equal to $\kappa^{1/3}$. Following this line of reasoning, we can postulate some polygonal "analogues" of Eq. (1).

To go from $\kappa^{1/3}\vec{\mathcal{N}}$, represented by the evolution to the local center of mass, to $\kappa\vec{\mathcal{N}}$, we choose two different approaches:

1. Change the length of the evolution vector (from each vertex toward the local center of mass), which presumably is $\kappa^{1/3}$, to its third power. Figure 13(a). shows some experimental results of this approach. We observed experimentally that arbitrary initial polygons converged to regular polygonal disks. In fact, we observed that any power greater than one gives the same result. This "strange" result seems to be similar to a recent result of Alvarez *et al.*[2] who found that from the evolutions

   $$\mathcal{C}_t = \kappa^{\alpha}\vec{\mathcal{N}},$$

   only the evolution with $\alpha = \frac{1}{3}$ is affine invariant (see also Refs. 32 and 33). All others are naturally Euclidean invariant evolutions.

2. Assume that the external angle is a local measure of the "discrete curvature" at the vertex. Then, we are led to multiply the vector given by the evolution towards the local center of mass, by the value of the external angle, taken to the 2/3 power. Experimental results are shown in Fig. 13(b). Again, convergence to a regular polygonal approximation of a circle was obtained. In fact, the same behavior was observed for several monotonically ascending functions of the angle.

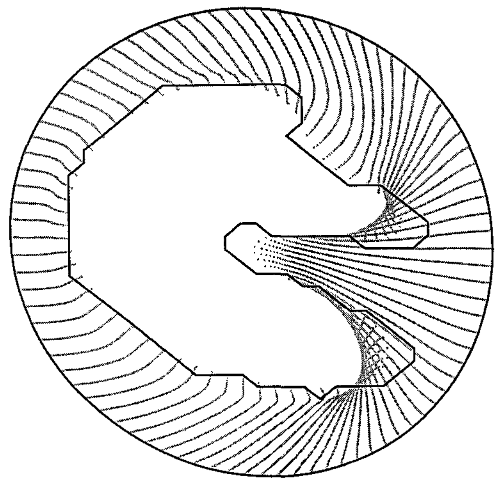

(a)

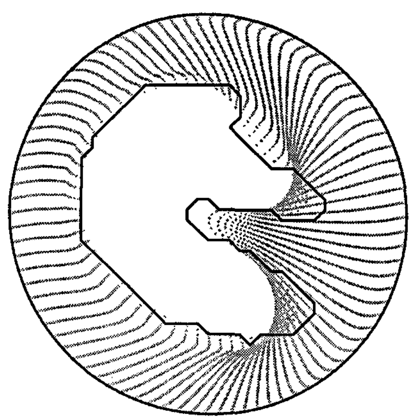

(b)

Fig. 13. Examples of the second polygonal Euclidean shortening model. (The polygons are normalized at each step.) (a) Taking the third power. (b) Multiplying by the value of the external angle.

4. CONCLUDING REMARKS

In this paper, evolutions of closed planar *polygons* were studied. An advantage of the study of polygonal evolutions is that they are readily implemented on digital computers, and it is not necessary to deal with numerical algorithms similar to those developed for general curve evolution.[28]

The first part of the paper was devoted to linear evolutions. Due to linearity, these evolutions are inherently *affine-invariant* when the evolution matrix M is real. The general theory of such evolutions was presented, and two specific problems were analyzed, the first one being a polygonal version of the *affine shortening flow* recently described in Refs. 31 and 32. In this case, convergence to *polygonal ellipses* was proven. The second problem analyzed is related to cyclic pursuit,[8] and convergence, either to *polygonal ellipses* or to *polygonal circles*, was proven. Other cases can be analyzed using the described general theory, and a methodology similar to the one used for analyzing these two examples.

Together with the implementation advantage already mentioned, the described linear discretization of evolutions has the following main advantages as well:

1. The evolution is governed by a circulant matrix transformation.
2. The convergence analysis is simple and assumptions, like convexity or non self intersecting, become unnecessary.

We point out that the results of Sec. 2 for the general linear model with real evolution matrix (the affine invariant case), are not new. Prof. Gil Kallai from the Hebrew University in Jerusalem pointed out to us that M. G. Darboux considered in 1878 the following problem[13]:

> *"Considérons un polygone plan ou gauche de n côtés $A_1, A_2, \ldots, A_n$. On forme un second polygone de même nombre de côtés en joignant les milieux $A_1^{'}$, $A_2^{'}$, ..., $A_n^{'}$ des côtés $A_1A_2, \ldots, A_n$ du premier. De ce deuxième polygone on déduit un troisième par la même loi, puis un quatrième, et, en continuant indéfiniment, on obtain ainsi une suite illimitée de polygones. Je me propose de démontrer que ces polygones deviennent de plus en plus petits, c'est-à-dire que tous les sommets du polygons de rang n de la série précédente se rapprochent d'un point fixe quand n croit indéfiniment; et, en même temps, je déterminerai la forme de ce polygone quand il devient infiniment petit..."*

Therefore, Darboux studied the cyclic pursuit problem described in Sec. 2.3, for $c = \frac{1}{2}$. He also mentioned that the results are identical for different real values of c, and for evolution toward the local center of mass (as studied in Sec. 2.2).[13]

Subsequently, long after the results by Darboux were forgotten, other researchers re-discovered some of these results. Among them we mention I. J. Schoenberg in 1950,[34] J. H. Cadwell in 1953,[9] E. R. Berlekamp *et al.* in 1965,[5] L. Fejes Tóth in 1969.[16] Motivated by the search of discrete analogues of the affine invariant curve evolution presented in Refs. 31 and 32, we joined this list recently. Many other researchers worked on this and related problems connecting Fourier analysis with basic geometry.[6,11,12,15,23,26,27,35,37,39]

The second part of the paper was dedicated to the description of two possible approaches for polygonal analogues of the *Euclidean curve shortening flow*. The first approach is based on a definition of *polygonal curvature*. The second one is derived from the polygonal analog of the *affine shortening flow*. Experimental results show that when arbitrary initial polygons evolve according to the proposed models, they converge to polygonal approximations of circles.

Since we are dealing with polygonal analogues, the fact that the two models are different does not contradict the hypothesis that perhaps both models are correct analogues of the Euclidean shortening. Of course, experimental results are not enough, and it will be nice to also have theoretical proofs of these results.

These initial results on the evolution of polygons, pose a large number of interesting related questions. Besides the challenge to find proofs for the Euclidean models, it would be very interesting to find the analogues of some other continuous evolutions which were also found to be very important both from the theoretical and the practical point of view. These and other topics concerning projective invariance, were already and are still under investigation. See for example Ref. 40 and the references therein.

ACKNOWLEDGMENT

The authors thank Prof. Allen Tannenbaum for many interesting discussions on evolutions, mathematics, and life in general, Prof. Gil Kallai for pointing out the old results by Darboux, Prof. Sanjeev Kulkarni for proposing the model in Sec. 3.1, and Dr. Tom Richardson for some very interesting insights on discrete Euclidean evolutions.

REFERENCES

1. L. Alvarez, P. L. Lions, and J. M. Morel, "Image selective smoothing and edge detection by nonlinear diffusion II", *SIAM J. Numer. Anal.* **29** (1992) 845–866.
2. L. Alvarez, F. Guichard, P. L. Lions, and J. M. Morel, "Axiomatisation et nouveaux operateurs de la morphologie mathematique", *C. R. Acad. Sci. Paris* **315** (1992) 265–268.
3. S. Angenent, "Parabolic equations for curves on surfaces, Part I. Curves with p-integrable curvature", *Annals Mathematics* **132** (1990) 451–483.
4. S. Angenent, "Parabolic equations for curves on surfaces, Part II. Intersections, blow-up, and generalized solutions", *Annals of Mathematics* **133** (1991) 171–215.
5. E. R. Berlekamp, E. N. Gilbert, and F. W. Sinden, "A polygon problem", *The American Mathematical Monthly* **72** (1965) 233–241.
6. M. Bourdeau and S. Dubuc, "L'tération de Fejes Tóth sur un polygone", *J. Geom.* **6** (1975) 65–75.
7. A. M. Bruckstein and A. N. Netravali, "On differential invariants of planar curves and recognizing partially occluded planar shapes", *AT&T Technical Report*, July 1990, also to appear in the *Proc. Visual Form Workshop*, Capri, May 1991, Plenum Press.
8. A. M. Bruckstein, N. Cohen, and A. Efrat, "Ants, crickets and frogs in cyclic pursuit", CIS Report #9105, Department of Computer Science, Technion, I. I. T., Haifa 32000, Israel, 1991.

9. J. H. Cadwell, "A property of linear cyclic transformations", *Math. Gaz.* **37** (1953) 85–89.
10. M. P. Do Carmo, *Differential Geometry of Curves and Surfaces*, Prentice-Hall, Inc., New Jersey, 1976.
11. R. J. Clarke, "Sequences of polygons", *Math. Mag.* **52** (1979) 102–105.
12. P. J. Davis, "Cyclic transformations of polygons and the generalized inverse", *Can. J. Math.* **39** (1977) 756–770.
13. M. G. Darboux, "Sur un probleme de geometrie elementaire", *Bull. Sci. Math.* **2** (1878) 298–304.
14. C. L. Epstein and M. Gage, "The curve shortening flow", in *Wave Motion: Theory, Modeling, and Computation*, A. Chorin and A. Majda, eds., Springer-Verlag, New York, 1987.
15. G. Fejes Tóth, "Iteration processes leading to a regular polygon", *Mat. Lapok* **23** (1970) 135–141, (in Hungarian).
16. L. Fejes Tóth, "Iteration methods for convex polygons", *Mat. Lapok* **20** (1969) 15–23, (in Hungarian).
17. M. Gage, "Curve shortening makes convex curves circular", *Invent. Math.* **76** (1984) 357–364.
18. M. Gage and R. S. Hamilton, "The heat equation shrinking convex plane curves", *J. Differential Geometry* **23** (1986) 69–96.
19. R. C. Gonzalez and P. Wintz, *Digital Image Processing*, Addison-Wesley, Reading, Massachusetts, 1987.
20. M. Grayson, "The heat equation shrinks embedded plane curves to round points", *J. Differential Geometry* **26** (1987) 285–314.
21. M. Grayson, "Shortening embedded curves", *Annals of Mathematics* **129** (1989) 71-111.
22. H. W. Guggenheimer, *Differential Geometry*, McGraw-Hill Book Company, New York, 1963.
23. F. Kárteszi, "A pair of affinely regular pentagons generated from a convex pentagon", *Mat. Lapok* **20** (1969) 7–13, (in Hungarian).
24. B. B. Kimia, A. Tannenbaum, and S. W. Zucker, "Toward a computational theory of shape: An overview", *Lecture Notes in Computer Science,* Vol. 427, Springer-Verlag, New York, 1990, pp. 402–407.
25. M. S. Klamkin, "Cyclic pursuit with lead angle", *SIAM Rev.*, **32**, 4 (1990) 673–674.
26. G. Korchmáros, "An iteration process leading to affinely regular polygons", *Mat. Lapok* **20** (1969) 405–401, (in Hungarian).
27. G. Lükó, "Certain sequences of inscribed polygons", *Period. Math. Hungar.* **3** (1973) 255–260.
28. S. J. Osher and J. A. Sethian, "Fronts propagation with curvature dependent speed: Algorithms based on Hamilton-Jacobi formulations", *Computational Phys.* **79** (1988) 12–49.
29. S. Osher and L. I. Rudin, "Feature-oriented image enhancement using shock filters", *SIAM J. Numer. Anal.* **27** (1990) 919–940.
30. G. Sapiro, R. Kimmel, D. Shaked, B. B. Kimia, and A. M. Bruckstein, "Implementing continuous-scale morphology via curve evolution", *Pattern Rec.* **26** (1993) 1363–1372.
31. G. Sapiro and A. Tannenbaum, "On affine plane curve evolution", *J. Functional Analysis* **119** (1994) 79–120.
32. G. Sapiro and A. Tannenbaum, "Affine shortening of non-convex planar curves", EE Publication **845**, Department of Electrical Engineering, Technion, I. I. T., Haifa 32000, Israel, Aug. 1992.

33. G. Sapiro and A. Tannenbaum, "Affine invariant scale-space", *Int. J. of Computer Vision* **11** (1993) 25–44.
34. I. J. Schoenberg, "The finite Fourier series and elementary geometry", *Amer. Math. Monthly* **57** (1950) 390–404.
35. D. B. Shapiro, "A periodicity problem in plane geometry", *Amer. Math. Monthly* **99** (1984) 97–108.
36. M. Spivak, *A Comprehensive Introduction to Differential Geometry*, Publish or Perish Inc., Berkeley, California, 1979.
37. A. Szép, "Linear iterations of polygons", *Mat. Lapok* **21** (1970) 255–260, (in Hungarian).
38. B. White, "Some recent developments in differential geometry", *The Mathematical Intelligencer* **11**, 4 (1989) 41–47.
39. E. T. H. Wong, "Polygons, circulant matrices and Moore-Penrose inverses", *Amer. Math. Monthly* **88** (1981) 509–515.
40. A. H. Bruckstein and D. Shaked, "On projective invariant smoothing and evolution of planar curves and polygons", accepted in *J. Mathematical Imaging and Vision*.

Received 23 December 1993.

Guillermo Sapiro received his B. Sc. (summa cum laude), M. Sc., and Ph. D. from the Department of electrical engineering at the Technoin, Israel Institute of Technology, in 1989, 1991, and 1993, respectively. After post-doctoral research at MIT, Dr. Sapiro recently became a Member of Technical Staff at the research facilities of HP Labs in Palo Alto, California. He works on differential geometry and geometric partial differential equations, both in theory and applications in computer vision and image analysis.

Doron Shaked graduated from the Electrical and Computer Engineering Department of the Ben Gurion University in Beer Sheva, Israel in 1988 and received the M. Sc. and D. Sc. from the Electrical Engineering Department of the Technion, in Haifa, Israel in 1991 and 1995, respectively. Currently he is with Hewlett Packard, Israel Science Center. His research interests include computer vision, pattern recognition, shape analysis, axial shape representation and thinning algorithms and sequential decision theory.

Alfred M. Bruckstein received the B. Sc. and M. Sc. degrees in electrical engineering, from the Technion, Israel Institute of Technology, in 1977 and 1980, respectively, and Ph.D. degree in electrical engineering from Stanford University, Stanford, California, in 1984.

From October 1984, he has been with the Technion, Haifa, Israel. He is a frequent visitor at AT&T's Bell Laboratories, Murray Hill, New Jersey (where he presently is on sabbatical). His present research interests are in computer vision, pattern recognition, image processing, and computer graphics. He has also done work in estimation theory, signal processing, algorithmic aspects of inverse scattering, point processes and mathematial models in neurophysiology.